Optical Materials 68 (2017) 7–10

Contents lists available at ScienceDirect

Optical Materials

journal homepage: www.elsevier.com/locate/optmat

Luminescence investigation of Ce incorporation in garnet-type $Li_7La_3Zr_2O_{12}$

A.A. Trofimov, C. Li, K.S. Brinkman, L.G. Jacobsohn*

Department of Materials Science and Engineering, Clemson University, Clemson, SC 29634, USA

ARTICLE INFO

Article history:
Received 30 August 2016
Accepted 19 September 2016
Available online 28 September 2016

Keywords:
Garnet
Cerium
Radioluminescence
Thermal quenching

ABSTRACT

The effects of the incorporation of Ce on the luminescence of tetragonal garnet-type $Li_7La_3Zr_2O_{12}$ (LLZO) were examined. Undoped and Ce-doped LLZO powders with nominal compositions of $Li_7(La_{1-x}Ce_x)_3Zr_2O_{12}$ with x = 0, 0.005, 0.01, 0.03, and 0.05 were synthesized via conventional solid state reaction. X-ray diffraction (XRD) revealed the structural evolution from tetragonal to cubic LLZO, together with Li_2ZrO_3 and Ce_4O_7 minor phases upon Ce incorporation. Undoped LLZO exhibited a single luminescence band centered at 2.84 eV that was quenched by the incorporation of Ce. A Gaussian band deconvolution analysis of the radioluminescence (RL) spectra suggested that Ce occupied two distinct crystallographic sites when replacing for La, with emission bands centered at 2.41 and 2.78 eV. The Gaussian band deconvolution analysis of RL spectra up to ~250 °C revealed thermal quenching reduced the intensity by about half at 50–60 °C, with negligible emission detected at about 250 °C.

1. Introduction

There has been continuous effort directed to the discovery and development of new scintillators [1,2]. Ce- or Pr-doped garnets have been among the most investigated scintillators, both in the form of single crystals and polycrystalline ceramics. A Ce-doped $Y_3Al_5O_{12}$ (YAG:Ce) scintillator was first reported in the mid-1970's [3], while the first reports on LuAG based scintillators appeared in the mid-1990's [4]. Later, this research thrust included Ce-doped multicomponent garnets $(Y,Gd)_3(Ga,Al)_5O_{12}$ and $(Lu,Gd)_3(Ga,Al)_5O_{12}$ [5,6]. In this work, this research is further expanded to include multicomponent garnet-type material $Li_7La_3Zr_2O_{12}$ (LLZO). This material has been suggested as a promising solid-state electrolyte for lithium ion batteries as a substitute for current liquid electrolyte and polymer based separators targeting enhanced operational safety. However, the luminescent properties of undoped and Ce-doped LLZO are mostly unexplored [7]. In this work, a systematic investigation of effect of the incorporation of Ce into LLZO was carried out with particular emphasis on its luminescent properties.

2. Experimental procedure

Undoped and Ce-doped LLZO powders with a nominal composition of $Li_7(La_{1-x}Ce_x)_3Zr_2O_{12}$ with x = 0, 0.005, 0.01, 0.03, and 0.05 were synthesized via the conventional solid state route with the following starting materials: Li_2CO_3 (Macron Fine Chemicals; 99.9%), La_2O_3 (Alfa Aesar; 99.99%), ZrO_2 (Alfa Aesar; 99.7%), and cerium(III) ammonium nitrate tetrahydrate (Alfa Aesar; reagent purity). The precursor powders were ball-milled for 24 h using yttrium stabilized zirconia (YSZ) grinding balls, followed by calcination in sealed alumina crucibles at 950 °C for 5 h in a box furnace. The ball-milling and calcination steps were repeated a total of 3 times in order to obtain powders with single phase.

X-ray diffraction (XRD) measurements were carried out with a Rigaku AFC-7R (18 kW) diffractometer using CuKα radiation in the 10°–70° 2θ range with 1°/min scanning rate at ambient conditions.

Radioluminescence (RL) measurements were carried out as a function of the temperature, from room temperature (RT) up to 250 °C, using a custom-designed Lexsyg Research spectrofluorometer by Freiberg Instruments equipped with an Andor Technology DU920P-BU Newton CCD camera, and a Varian Medical Systems VF-50J X-ray tube with a W target and operated at 40 kV and 1 mA. Spectra were not corrected for the spectral response of the system. Spectral analysis was carried out by means of Gaussian band deconvolution.

* Corresponding author.
E-mail address: luiz@clemson.edu (L.G. Jacobsohn).

http://dx.doi.org/10.1016/j.optmat.2016.09.058
0925-3467/

3. Results and discussion

Fig. 1 shows XRD results of undoped and Ce-doped LLZO with $0 \leq x \leq 0.05$ that revealed the structural evolution of LLZO upon Ce incorporation. Undoped LLZO has tetragonal structure (183684-ICSD; [8]) composed of $La(1)O_8$ and $La(2)O_8$ dodecahedra, ZrO_6 octahedra, and Li octahedra and tetrahedra [9]. Up to about $x = 0.01$, the host remained essentially tetragonal LLZO though minor distortions in the diffraction peaks could be observed. Further Ce incorporation led to structural changes that culminated in a different structure for $x = 0.05$ that corresponded to a combination of cubic LLZO (261302-ICSD; [10]), and a secondary phase Ce_4O_7 (PDF#:65-7999). Li_2ZrO_3(PDF#:330843) was also observed as a secondary minor phase.

Fig. 2 summarizes the RL results at room temperature. Undoped and Ce-doped LLZO presented broad emission bands within the spectral range of about 2–3.5 eV. Incorporation of Ce changed the emission spectra, with the centroid shifting to lower energies compared to undoped LLZO. Spectra of LLZO with Ce content up to $x = 0.03$ were similar in shape and spectral range, while for $x = 0.05$ a distinct spectrum shifted to even lower energies was observed. Spectral analysis by means of Gaussian bands deconvolution (dotted lines) revealed the emission spectrum of undoped tetragonal LLZO to be composed of a single band centered at 2.84 eV. This band had been reported before and attributed to the Zr-O charge transfer (CT) transition [7]. At room temperature, within the $0.005 \leq x \leq 0.03$ compositional range, the spectra were deconvoluted with two Gaussian bands (dotted lines) centered at about 2.41 and 2.78 eV, and for $x = 0.05$ an additional band centered at about 2.15 eV was necessary to achieve reliable spectral deconvolution. The behavior of the peak position of the individual Gaussian bands is presented in Fig. 3a and showed that Ce incorporation into LLZO quenched the intrinsic Zr-O CT transition, and that Ce occupied two distinct crystallographic sites, as expected from its substitution for La. The difference in energy of 0.37 eV between the two emission bands in tetragonal LLZO:Ce is in very good agreement with the difference observed between the emission bands of Ce^{3+} in two distinct crystallographic sites in Gd_2SiO_5 [11], while being too high to be attributed to spin-orbit splitting typically on the order of 0.25 eV. Fig. 3b presents the 2.41/2.78 integrated band intensity ratio. The behavior of the intensity ratio as a function of the Ce

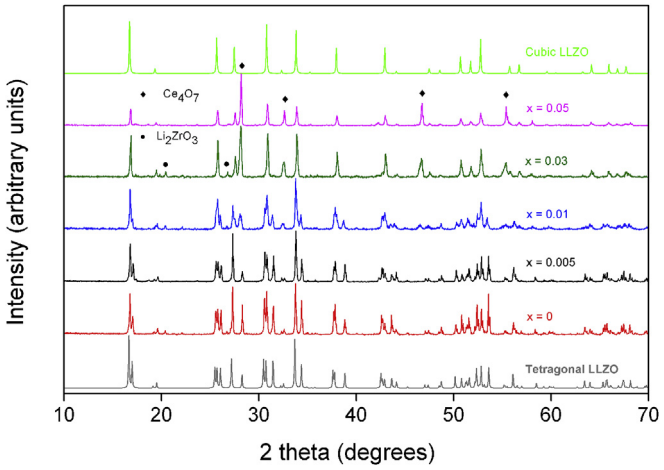

Fig. 1. XRD results of $Li_7(La_{1-x}Ce_x)_3Zr_2O_{12}$ with $x = 0$, 0.005, 0.01, 0.03, and 0.05, together with calculated diffractograms of cubic and tetragonal LLZO based on 261302-ICSD [10] and 183684-ICSD [8], respectively. The position of the diffraction peaks from minor phases are indicated. Diffractograms were shifted vertically to improve visual clarity.

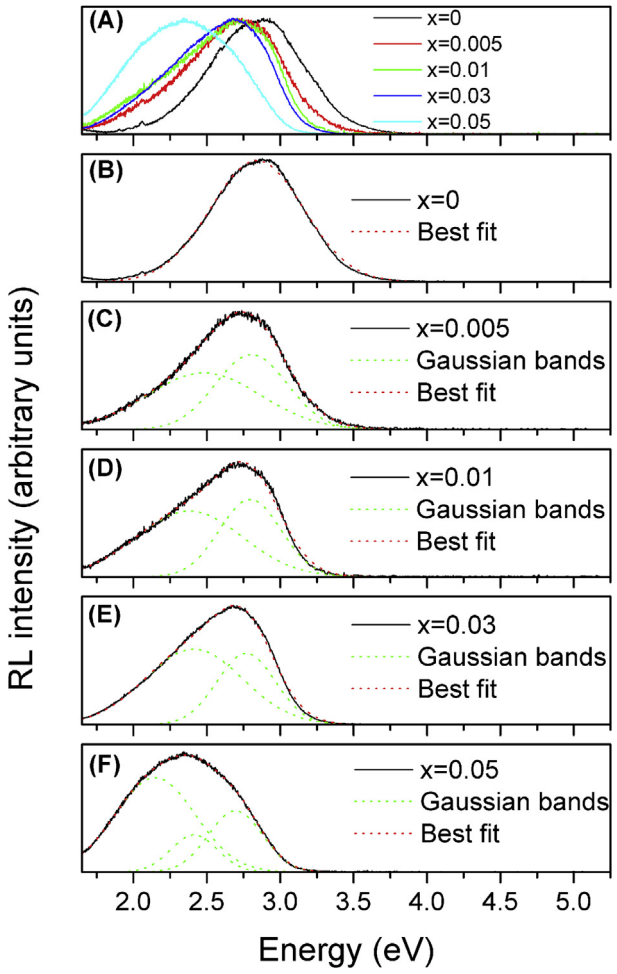

Fig. 2. a) Normalized RL spectra of $Li_7(La_{1-x}Ce_x)_3Zr_2O_{12}$ with $x = 0$, 0.005, 0.01, 0.03, and 0.05 obtained at room temperature. Gaussian band deconvolution of RL spectra for b) $x = 0$, c) $x = 0.005$, d) $x = 0.01$, e) $x = 0.03$, and f) $x = 0.05$.

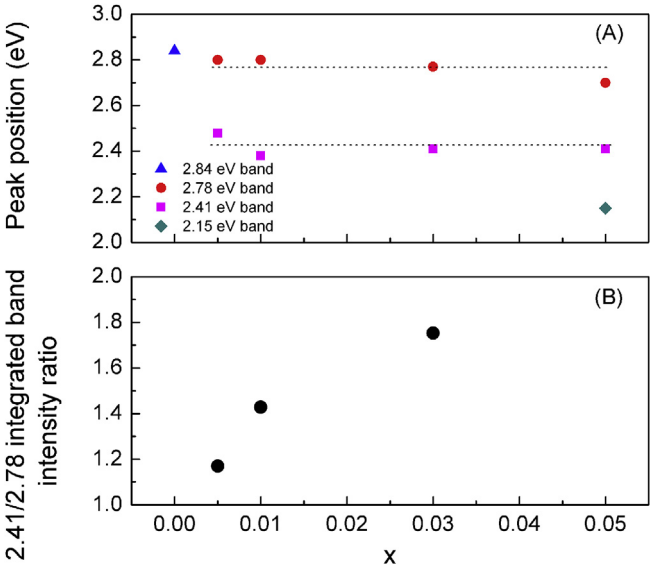

Fig. 3. a) Peak position of Gaussian bands used in the deconvolution of RL spectra obtained at room temperature, and b) 2.41/2.78 integrated band intensity ratio as a function of the nominal Ce content.

content suggested an increasing preference for Ce to be incorporated into the site responsible for the band located at 2.41 eV. Since the ionic radius of La^{3+} is slightly larger than of Ce^{3+} [12], and since the La-O distances are overall longer in $La(1)O_8$ than in the $La(2)O_8$ sites [9], easier incorporation of Ce^{3+} into $La(1)O_8$ sites is expected suggesting the 2.41 eV band is associated with Ce^{3+} occupying these sites. The band at 2.15 eV is attributed to Ce emission in cubic LLZO.

The effects of temperature on RL are presented in Fig. 4 for x = 0, 0.005, and 0.01 for selected temperatures between room temperature and 250 °C. Already by 50–60 °C, thermal quenching reduced intensity by about half. At 250 °C the emission was negligible for undoped LLZO and weak for the Ce-doped materials, with higher Ce contents yielding higher thermal stability. In Fig. 5, the results of the spectral deconvolution are presented as a function of temperature. Similarly to the room temperature data, the emission from undoped LLZO was fit with one Gaussian band while for x = 0.005 and 0.01 two bands were used. Fig. 5a shows the evolution of the peak position of the Gaussian bands as a function of the temperature. The band centered at 2.84 eV (at room temperature) observed only in undoped tetragonal LLZO showed a small shift toward lower energies, from 2.84 to 2.82 eV. In the case of x = 0.005 and 0.01, both bands shifted to lower energies, from 2.78 to 2.34 eV and from 2.41 to 1.95 eV (average values), respectively, over the entire temperature range, with the 2.41 eV band stabilizing at 1.95 eV at about 150 °C. Fig. 5b shows the 2.41/2.78 integrated band intensity ratio

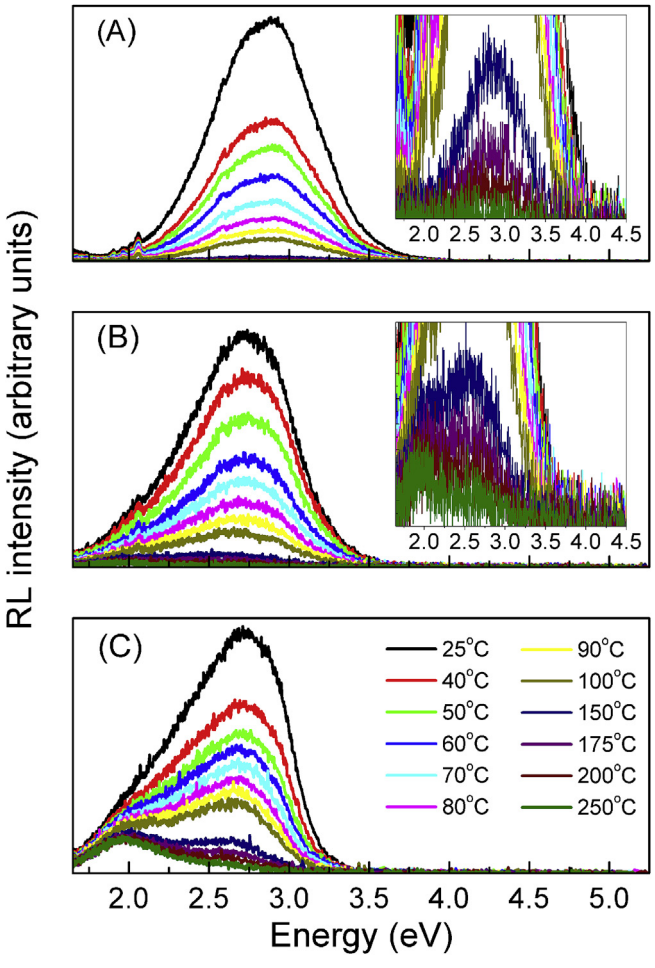

Fig. 4. RL spectra obtained at different temperatures for a) x = 0, b) x = 0.005, and c) x = 0.01. The color indicates the temperature at which the spectrum was taken.

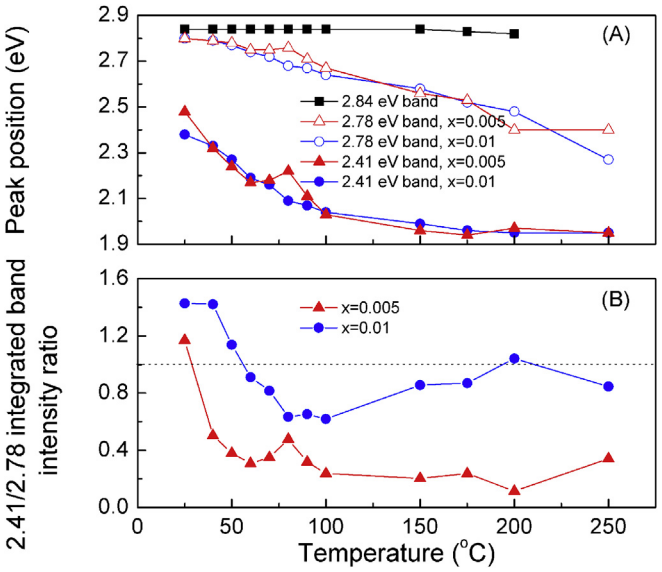

Fig. 5. Results of Gaussian band spectral deconvolution as a function of temperature for x = 0.005, and 0.01: a) peak position, and b) integrated band intensity ratio.

for LLZO with x = 0.005 and 0.01 as a function of the temperature. These results show that while luminescence is dominated by the emission of the 2.41 eV band at room temperature/low temperatures, depending on the Ce concentration, the center responsible for this emission is more strongly thermally quenched than the center responsible for the 2.78 eV band. Different thermal stability of Ce occupying nonequivalent crystallographic sites was also observed in Gd_2SiO_5:Ce [11]. The distinct thermal behavior of each of the emission bands centered at 2.84, 2.78, and 2.41 eV demonstrate the different nature of the respective luminescence centers associated to these bands.

4. Conclusions

An investigation of the effects of the incorporation of Ce on the luminescence of tetragonal LLZO was carried out. Ce incorporation led to progressive structural changes that ultimately transformed LLZO into its cubic polymorph. While undoped tetragonal LLZO presented a single emission band centered at 2.84 eV, Ce incorporation quenched the LLZO intrinsic emission concomitant to generating two distinct emission bands at 2.78 and 2.41 eV. These bands were attributed to Ce substituting for La in its two nonequivalent crystallographic sites, as revealed by spectral Gaussian band deconvolution. The different nature of these luminescence centers was further evidenced by means of RL measurements as a function of the temperature, when each emission band presented an unique thermal behavior. Significant thermal quenching was observed already at 50–60 °C, with higher Ce contents yielding higher thermal stability.

Acknowledgements

This material is based upon work supported by the National Science Foundation under Grant No. 1207080.

References

[1] W.W. Moses, Nuc. Instrum. Meth. Phys. Res. A 487 (2002) 123.
[2] S. Derenzo, G. Bizarri, R. Borade, E. Bourret-Courchesne, R. Boutchko, A. Canning, A. Chaudhry, Y. Eagleman, G. Gundiah, S. Hanrahan, M. Janecek, M. Weber, Nuc. Instrum. Meth. Phys. Res. A 652 (2011) 247.

[3] R. Autrata, P. Schauer, J. Kvapil, J. Kvapil, J. Phys. E Sci. Instrum. 11 (1978) 707.
[4] M. Nikl, A. Yoshikawa, K. Kamada, K. Nejezchleb, C.R. Stanek, J.A. Mares, K. Blazek, Prog. Cryst. Growth Charac. Mater 59 (2013) 47.
[5] K. Kamada, T. Yanagida, J. Pejchal, M. Nikl, T. Endo, K. Tsutumi, Y. Fujimoto, A. Fukabori, A. Yoshikawa, J. Phys. D. Appl. Phys. 44 (2011) 505104.
[6] K. Kamada, T. Endo, K. Tsutumi, T. Yanagida, Y. Fujimoto, A. Fukabori, A. Yoshikawa, J. Pejchal, M. Nikl, Cryst. Growth Des. 11 (2011) 4484.
[7] X. Zhang, Z. Zhang, S.I. Kim, Y.M. Yu, H.J. Seo, Cer. Inter 40 (2014) 2173.
[8] A. Logeat, T. Koohler, U. Eisele, B. Stiaszny, A. Harzer, M. Tovar, A. Senyshyn, H. Ehrenberg, B. Kozinsky, Solid State Ionics 206 (2012) 33.
[9] J. Awaka, N. Kijima, H. Hayakawa, J. Akimoto, J. Sol. State Chem. 182 (2009) 2046.
[10] C.A. Geiger, E. Alekseev, B. Lazic, M. Fisch, T. Armbruster, R. Langner, M. Fechtelkord, N. Kim, T. Pettke, W. Weppner, Inorg. Chem. 50 (2011) 1089.
[11] H. Suzuki, T.A. Tombrello, C.L. Melcher, J.S. Schweitzer, Nuc. Instrum. Meth. Phys. Res. A 320 (1992) 263.
[12] R.D. Shannon, Acta Crystallogr. A 32 (1976) 751.